Preparation by melt mixing and characterization of isotactic polypropylene/SiO2 nanocomposites containing untreated and surface-treated nanoparticles

ARTICLE *in* JOURNAL OF APPLIED POLYMER SCIENCE · MAY 2006

Impact Factor: 1.77 · DOI: 10.1002/app.22849

6 AUTHORS, INCLUDING:

Dimitrios N Bikiaris
Aristotle University of Thessaloniki
297 PUBLICATIONS **6,991** CITATIONS
SEE PROFILE

Eleni Pavlidou
Aristotle University of Thessaloniki
208 PUBLICATIONS **2,703** CITATIONS
SEE PROFILE

N. Vouroutzis
Aristotle University of Thessaloniki
69 PUBLICATIONS **578** CITATIONS
SEE PROFILE

George P. Karayannidis
Aristotle University of Thessaloniki
77 PUBLICATIONS **1,759** CITATIONS
SEE PROFILE

Preparation by Melt Mixing and Characterization of Isotactic Polypropylene/SiO_2 Nanocomposites Containing Untreated and Surface-Treated Nanoparticles

Dimitris N. Bikiaris,[1] George Z. Papageorgiou,[1] Eleni Pavlidou,[2] Nikolaos Vouroutzis,[2] Paraskevas Palatzoglou,[3] George P. Karayannidis[1]

[1]*Laboratory of Organic Chemical Technology, Department of Chemistry, Aristotle University of Thessaloniki, 541 24 Thessaloniki, Macedonia, Greece*
[2]*Department of Physics, Aristotle University of Thessaloniki, 541 24 Thessaloniki, Macedonia, Greece*
[3]*Karina ABEE Plastics Industry, New Santa Kilkis, 545 00 Kilkis, Macedonia, Greece*

Received 24 September 2004; accepted 12 May 2005
DOI 10.1002/app.22849
Published online 9 February 2006 in Wiley InterScience (www.interscience.wiley.com).

ABSTRACT: In the present study two series of isotactic polypropylene (iPP)/SiO_2 nanocomposites containing 1, 2.5, 5, 7.5, and 10 wt % SiO_2 nanoparticles were prepared by melt-mixing on a twin-screw corotating extruder. In the first series untreated fumed silica nanoparticles were used, whereas in the second nanoparticles were surface-treated with dimethyldichlorosilane. In both cases, the average size of the primary nanoparticles was 12 nm. Tensile and impact strength were found to increase and to be affected mainly by the type and content of silica nanoparticles. A maximum was observed, corresponding to samples containing 2.5 wt % SiO_2. These findings are discussed in light of the SEM and TEM observations. By increasing the amount of nanoparticles, large aggregates of fumed silica could be formed, which may explain the reduction of mechanical properties with higher concentrations of SiO_2. However, it was found that surface-treated nanoparticles produced larger aggregates than did those derived from untreated nanoparticles, despite the increased adhesion of the iPP matrix, as was postulated from yield strength. This behavior negatively affected mechanical properties. In addition, an effort was made to determine if toughening theories, mainly the critical interparticle distance for rubber toughening or composites, also might be applicable in nanocomposites. From DSC measurements it was demonstrated that silica nanoparticles acted as effective nucleating agents, increasing the crystallization rate and the degree of crystallinity of iPP. © 2006 Wiley Periodicals, Inc. J Appl Polym Sci 100: 2684–2696, 2006

Key words: isotactic polypropylene; silica; nanocomposites; tensile properties; thermal properties; morphology

INTRODUCTION

Minerals have been added to thermoplastic polymers since the 1930s for various reasons, mainly to reduce the cost of the end products (fillers) because many fillers, especially calcium carbonate, have spectacular low-volume costs compared to thermoplastics. The term *mineral fillers* also has been used fairly broadly to include any particulate material, whether inorganic, natural, or synthetic in origin, as short glass fibers.[1] However, it had been demonstrated that fillers play substantial roles in modifying the properties of various thermoplastics, and it has been proved that the addition of these fillers is an effective way to improve the mechanical properties of polymeric materials. Because of this enhancement, reducing cost has become less important, and the attention of researchers has been focused on the improvement in properties that could be achieved by the addition of filler. Several factors influencing the processability and mechanical properties of polymer composites must be taken into account. These include the amount of added filler, the average particle size, interactions between fillers and polymer matrix, as well as interactions between filler particles themselves, yielding strong agglomerations.[2–8] After the introduction of filler, some polymer properties such as stiffness, heat deflection temperature, dimension stability, and flammability are improved, whereas the effect on others, especially toughness, is detrimental.

Traditional fillers such as calcium carbonate, talk, mica, silica, alumina, and magnesium hydroxide require high loading in order to achieve improved performance. However, an increase in the weight of the final product is undesirable, compared with light polymers. To overcome this drawback, in the last few years a new class of mineral-reinforced thermoplastics known as nanocomposites has been investigated. Fill-

Correspondence to: G. P. Karayannidis (karayan@chem.auth.gr).

Contract grant sponsor: Greek General Secretariat of Research and Technology under the research program PABE 2000.

ers in nanocomposites are nanometer sized, preferably less than 10 nm, providing miscibility with the polymer matrix and exploiting the unique synergism of the combined materials. Thus, the addition of such nanoparticles in thermoplastic resins offers many advantages, compared with traditional fillers, to create revolutionary materials. Because of high aspect ratios, nanoscopic filler particles produce an ultralarge interfacial area per volume with the polymer matrix. As a result, the nanocomposites produced show improvement in properties including toughness and impact performance, thermal stability, gas barrier properties, and electrical and thermal conductivity. The promise of industrial uses of such materials seems to be undiminished, especially in composite preparation. It could also have contributed to the renewed interest in toughness enhancement of thermoplastics with filler addition. Several published works have claimed that rigid particle fillers can increase polymer toughness in thermoplastic matrices like HDPE and PP.[9–14]

The traditional way that thermoplastics are reinforced involves the addition of the proper amount of rubber. The mechanism of achieving substantial absorption of the applied force is associated with rubber particle cavitation and shear yielding of the matrix. According to Dompas and Groeninckx, cavitation of rubber depends on its elastic and molecular properties, on the apparent volume strain, and on rubber particle size.[15] So, for cavitation, the critical size of particles has been estimated to range between 100 and 200 nm. Wu proposed another criterion for sufficient toughening, namely, critical interparticle distance,[16,17] whose value must be smaller than a predetermined critical value that is independent of rubber volume fraction and particle size. It is believed that interparticle distance is an inherent property of the matrix and that because van der Waals attractions provide sufficient adhesion for toughening, interfacial chemical bonding is not necessary. So, even with strong interfacial chemical bonding, a polymer/rubber blend will remain brittle if the interparticle distance is greater than the critical value. However, in related articles in the literature it was reported that significant deviations were found between values for critical ligament thickness, even in the same polymer. Thus, critical ligament thickness values of about 0.6 and 0.3 μm were reported for polyamide,[17] whereas for HDPE this property was found to be below 0.6 μm.[18] For isotactic polypropylene (iPP) the critical value was variously reported as about 0.15 μm[19] and less than 0.42 μm[20]; for polyoxymethylene (POM) as 0.18[21] and 0.56 μm[22]; for poly(phenylene sulfide) as 0.2 or 0.15 μm, depending on sample crystallinity[21]; for poly(butylene terephthalate) (PBT) as 0.16 and 0.4 μm depending on whether the copolymer was ethylene olefin rubber (EOR) or styrene-ethylene-butadiene-styrene (SEBS), respectively[21]; and for poly(ethylene terephthalate) as approximately 0.1 μm.[23]

Argon's research group has extended the criterion of interparticle distance beyond polymer/rubber toughening, proving that this property is intrinsic in each polymeric material and that instead of rubber, rigid mineral fillers like $CaCO_3$ can be used for semicrystalline polymer toughening.[9,24,25] This means that regardless of whether the material introduced into the polymer matrix is rubber or mineral filler, if the above criterion is satisfied, tough materials are produced. So this model can be used for the prediction of the supertough behavior of semicrystalline polymers modified not only with rubber particles but also with rigid inorganic fillers. Especially for nanocomposites, with the use of the proper amount of well-dispersed nanoparticles, supertough materials always should be formed. However, the basic issue is whether this theory is applicable in all cases when nanocomposites are used because, given the tiny size of the particles, the interparticle distance is always less than the previously reported values.

In the present work isotactic polypropylene (iPP) was used in order to prepare nanocomposites with SiO_2 nanoparticles. One of the most interesting commodity thermoplastics, iPP is used mainly for fiber production in the textile industry because it is cheaper and stronger than other synthetic fibers as film for food packaging, in bottle production, in tubes, and so forth. In the last few years, with the introduction of metallocene as a catalyst, higher isotacticity and narrow molecular weight distribution have been achieved. So, iPP with increased clarity, resistance to chemicals, durability to fatigue and abrasion, excellent recovery and enhanced mechanical properties has been produced. For this reason the worldwide production of iPP grew very fast, and there was a tendency to replace some of the used polymers, especially PVC and PS, in many of their applications. However, despite these advantages, the application of iPP also has a drawback. Although resistance to crack initiation is very high, in crack propagation it is very low, and when a crack or mechanical failure exists in the iPP matrix, it breaks very easily. To overcome this drawback, nanocomposites made up of several nanoparticles such as clay (montmorillonite), calcium carbonate, calcium phosphate, silver, and SiO_2 were prepared.[26–36]

In the present work silica nanoparticles were used because they are effective reinforcements for notch toughness and improvement of tensile performance of polypropylene[31,34,35] as well as for synthetic rubber.[37] SiO_2 nanoparticles are inherently hydrophilic, whereas the iPP polymer matrix is hydrophobic. For this reason, surface modification of nanoparticles is necessary in order to be compatible with such polymers. So in the present study surface-treated nano-

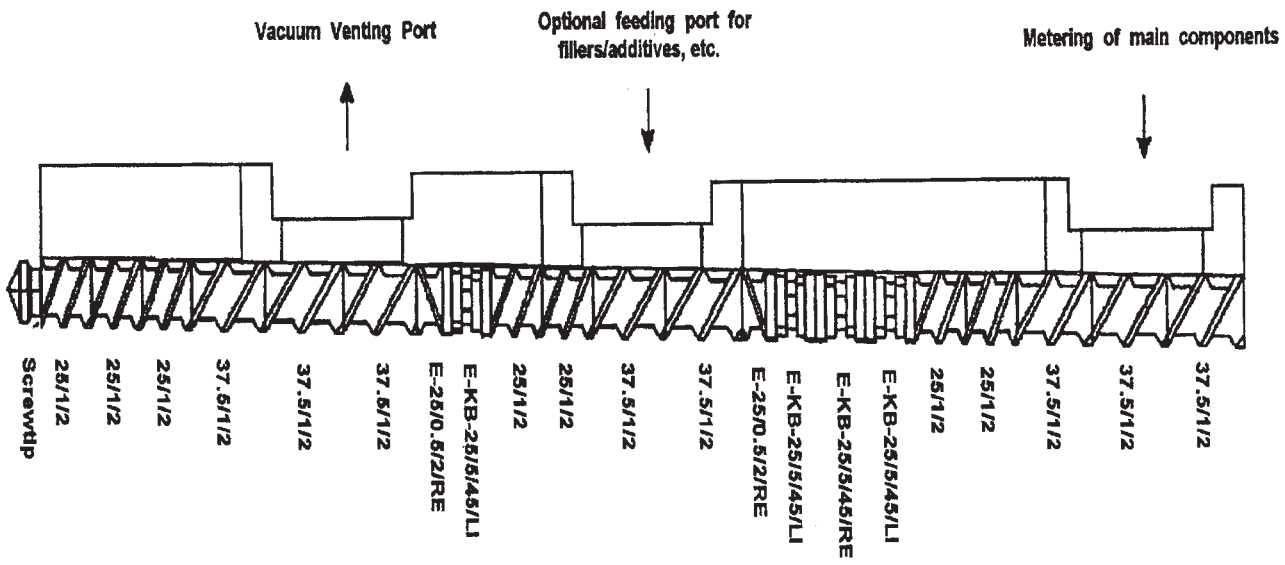

Figure 1 Screw configuration of corotating extruder used for nanocomposite preparation.

silica with dimethyldichlorosilane was used in order to increase the adhesion of the filler surface with the hydrophobic iPP matrix. These iPP/SiO_2 nanocomposites were compared with untreated SiO_2 nanoparticles.

EXPERIMENTAL

Materials

Isotactic polypropylene, supplied by Basell Polyolefines (Zaventem, Belgium), had a melt flow index (MFI) of 12 g/10 min at 190°C. The two types of fumed silica (SiO_2) nanoparticles used for nanocomposite preparation were supplied by Degussa AG (Hanau, Germany). The first type was the hydrophilic silica nanoparticle, under the trade name AEROSIL® 200, which had a specific surface area of 200 m^2/g and an SiO_2 content > 99.8%; the second type was the hydrophobic nanoparticle, under the trade name AEROSIL® R974. The latter was produced by the supplier after treating the hydrophilic nanoparticles with dimethyldichlorosilane. It had a lower specific surface than the untreated silica (170 m^2/g). Both types of silica nanoparticles had an average primary particle size of 12 nm.

Nanocomposite preparation

Nanocomposites containing 1, 2.5, 5, 7.5, and 10 wt % SiO_2 nanoparticles were prepared by melt-mixing on a Brabender (model DSC Φ25/32D) twin-screw corotating extruder (Fig. 1) with L/D 32 (D25 mm). Along the screw were different screw elements in order to induce polymer melting and to achieve fine dispersion of the nanoparticles in the polymer melt. The configurations and geometries of the different screw elements used for compounding are presented in Figure 1. The mixing section, after nanoparticle feeding, enhanced the compounding and also increased the residence time of the mixture in the barrel. Barrel pressure in this part, as well as in the metering section before the die, could be increased. The apparatus also had a vacuum vending port to remove any trace of moisture or other volatile products formed during compounding.

Prior to melt processing, silica nanoparticles were dried for 24 h at 105°C. The iPP pellets were fed into the throat of the extruder, whereas SiO_2 nanoparticles were introduced separately through a downstream-side feeding port into the polymer melt. Changing the feeding rate of each dosing unit automatically controlled the required proportions of both materials. Compounding was carried out using a screw rotating speed of 200 rpm and a temperature profile of 185°C, 195°C, 200°C, 200°C, 200°C, 195°C, and 185°C in the sequential heating zones from the hopper to the die. The melt temperature and pressure were continuously recorded during compounding. After compounding, the material was extruded from a die that had three cylindrical nozzles 4 mm in diameter in order to produce cylindrical extrudates. These were immediately immersed in a cold-water bath (20°C) and pelletized with an adjustable rotating knife located after the water bath into 5-mm lengths.

Differential scanning calorimetry

Thermal analysis of composites was performed using a differential scanning calorimeter (Perkin-Elmer, model Pyris 1, DSC) calibrated with metal standards.

For each measurement a sample of about 5 mg was used. It was placed in an aluminum pan that was sealed and heated to 200°C at a scanning rate of 20°C/min. To destroy all crystal nuclei and erase the previous thermal history, samples remained at this temperature for 5 min, after which they were quenched in the instrument to −60°C by cooling at the fastest cooling rate achieved. Fast cooling led to slightly lower crystallinity, and a second scan was performed up to 200°C at a heating rate of 20°C/min. From these scans the melting temperature (T_m) and the heat of fusion (ΔH_m) of the composites were measured. The crystallinity of the samples was calculated by using ΔH_m for pure crystalline iPP 165 J/g[38] after normalization of the ΔH_m composites to the amounts of iPP that they contained. For nonisothermal crystallizations samples were cooled at various cooling rates. Crystallization was performed at per-minute cooling rates of 2.5°C, 5°C, 10°C, and 20°C.

Mechanical properties

Measurement of mechanical properties such as tensile strength and elongation at break was performed on an Instron 1122 dynamometer in accordance with ASTM D638, using crosshead speeds of 5 and 50 mm/min. Izod impact testing was performed with a Tinius Olsen apparatus in accordance with ASTM D256. Prior to measuring, the samples were conditioned at 50% ± 5% relative humidity for 36 h by placing them in a closed chamber containing a saturated $Ca(NO_3)_2 \cdot 4H_2O$ solution in distilled water (ASTM E-104). Each sample was measured five times, and the results were averaged to obtain a mean.

The specimens for testing the mechanical properties were prepared in a single-screw injection machine by the Engel Company (Monomat 80, Germany) containing three heating zones. The temperature of each was 245°C, 195°C, or 190°C, from the feeding zone to the die, whereas the mold was cooled with water at 20°C.

Scanning electron microscopy

Scanning electron microscopy (SEM) was carried out a JEOL JMS-840A scanning microscope equipped with an energy-dispersive X-ray (EDX) Oxford ISIS 300 microanalytical system. For this purpose, fractured surfaces as well as thin films were used. All the studied surfaces were coated with carbon black in order to avoid charging under the electron beam.

Transmission electron microscopy

Electron diffraction (ED) and transmission electron microscopy (TEM) investigations were performed on variously modified samples deposited on copper grids. ED patterns and TEM micrographs were obtained using JEOL 120 CX microscope operating at 120 kV.

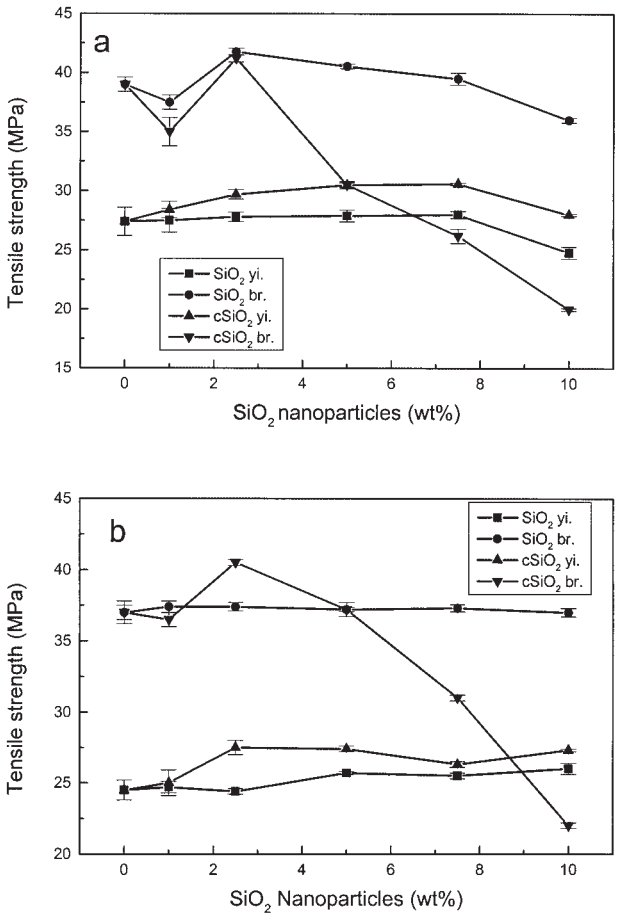

Figure 2 Tensile strength at the yield point and at the break of iPP and iPP/SiO_2 nanocomposites at crosshead speeds of (a) 50 mm/min and (b) 5 mm/min.

RESULTS AND DISCUSSION

Tensile properties and morphological characteristics

Tensile properties were measured in order to evaluate the reinforcing effect of nanoparticles into iPP. Because the nanoparticles in the iPP/SiO_2 nanocomposites had a very high surface area, it was expected that the applied stress would be easily transferred from the matrix into the silica particles, and so the mechanical properties would be enhanced. Figure 2 shows the variation in tensile strength of the iPP/SiO_2 nanocomposites containing untreated and surface-treated silica nanoparticles as a function of filler content. Tensile strength was measured applying the usual crosshead speed of 5 mm/min for composites, but also applying a speed of 50 mm/min. As can be seen in these diagrams, the measured values were greatly affected not only by the kind of silica and the silica content, but

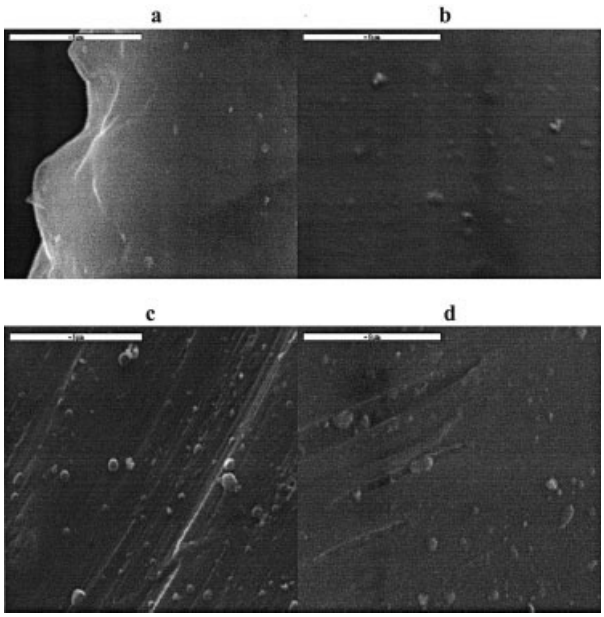

Figure 3 SEM micrographs of iPP/SiO_2 nanocomposites with different amounts of untreated SiO_2 after extension at a crosshead speed of 50 mm/min: (a) 1 wt %, (b) 2.5 wt %, (c) 5 wt %, (d) 10 wt %.

also by the crosshead speed. The samples extended at 50 mm/min showed superior mechanical properties. Tensile strength at break as well as at the yield point were both about 10%–20% higher for all nanocomposites compared to the corresponding values measured at a crosshead speed 5 mm/min.

A comparison of the nanocomposites containing treated and untreated particles showed that tensile strength at break increased in both cases for SiO_2 content up to 2.5 wt %, regardless of crosshead speed. For higher concentrations, a small reduction was observed in the samples with untreated silica, whereas a sharp decrease appeared for samples containing surface-treated particles. Rather, this reduction in tensile strength observed for SiO_2 higher than 5 wt % should be associated with the extended aggregation of silica nanoparticles, which, as was observed in micrographs, increased with increasing silica content. This finding was in agreement with a similar deterioration in mechanical properties reported for nylon-6/SiO_2 nanocomposites.[39] So, nanoparticle content seems to play an important role in how efficient they are as a reinforcement agent.

It is well known that filler dispersion and adhesion with the polymer matrix are of great importance in improving the mechanical behavior of composites. Fine control of the interface morphology of polymer nanocomposites is one of the parameters most critical to imparting the desired mechanical properties of such materials. To explain the behavior of the nanocomposites of this work, the surfaces of fractured specimens after drawing were examined with SEM (Figs. 3 and 4). In all the compositions the silica particles were spherical in shape, with the diameter dependent on the amount of SiO_2. For untreated samples the sizes detected by SEM were found to range between 100 and 330 nm with low silica content (up to 2.5 wt %). Increased sizes ranging between 100 and 550 nm were found with 5 wt % SiO_2, whereas with the highest silica content (10 wt %), particle sizes ranging from 120 to 750 nm were detected. From these micrographs it can be concluded that fumed silica created large agglomerates. However, in all the prepared nanocomposites the agglomerates did not exceed 1 μm in diameter. These results were in good agreement with the findings of Wu et al.,[31] who reported that increasing the content of untreated SiO_2 leads to larger agglomerates.

It can be seen that the silica agglomerates shown in Figure 3 are well distinguished. These micrographs also revealed that in most cases fracture resulted in complete debonding of silica nanoparticles from the surrounding iPP matrix because a rather smooth surface was left. This probably was an indication of poor interfacial adhesion between the two phases. For this reason, particle dispersion into the iPP matrix was not homogeneous. Voids created around the silica particles during extension were observed only when large particles had been formed as with 10 wt % SiO_2 and were not detected in nanocomposites with a low concentration of silica. According to Ash et al.,[40] only certain-sized particles initiated voids in poly(methyl methacrylate)/alumina nanocomposites. They also re-

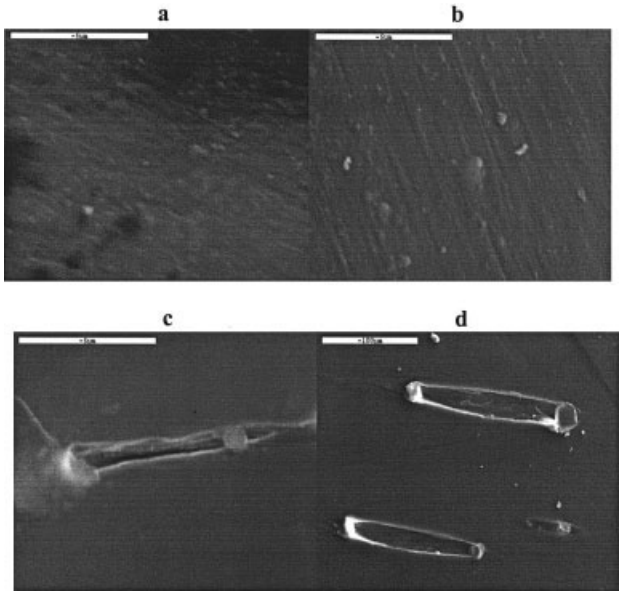

Figure 4 SEM micrographs of iPP/SiO_2 nanocomposites with different amounts of treated SiO_2 after extension at a crosshead speed of 50 mm/min: (a) 1 wt %, (b) 2.5 wt %, (c) 5 wt %, (d) 10 wt %.

ported that aggregates of smaller nanoparticles were aligned in the direction of the applied force. This was also the case in the iPP/SiO_2 nanocomposites in the present study, as shown in Figure 3(c).

Because hydrophilic fillers never have good adhesion with nonpolar polymers like iPP or adequate interactions in order to achieve fine dispersion, surface treatment is necessary to avoid agglomeration. So, the addition of surface-treated SiO_2 nanoparticles with dimethyldichlorosilane was expected to improve tensile strength because of better adhesion with iPP matrix. However, composites with treated SiO_2 content of more than 2.5 wt % exhibited an unexpected drop. SEM micrographs did not show noticeable evidence that the wetting of silica nanoparticles by the iPP matrix was improved by the coupling treatment with dimethyldichlorosilane (Fig. 4). In contrast, larger agglomerates were observed for nanocomposites with treated silica than for nanocomposites that were untreated. For a low content of silica, up to 2.5 wt %, the agglomerate diameter was smaller than 500 nm. With 5 and 7.5 wt % silica content, agglomerates of small diameters between 200 and 600 nm were observed as well as agglomerates with diameters up to 1 and 3 μm, respectively. With a 10 wt % content the agglomerates were up to 10 μm in diameter. At these silica contents, composites should be assumed to contain microparticles rather than nanoparticles. These clusters cause significant decrease in tensile strength and elongation at break because they consist of weak points, where fracture begins. For this reason, elongated cavities were clearly visible, with silica aggregations at the beginning of these cavities [Fig. 4(c,d)]. It is most probable that agglomerates were in the raw material because the specific surface was lower than that in untreated nanoparticles. Furthermore, the residence time of the materials in the extruder barrel during melt mixing was very low for destroying these agglomerates. It was calculated to be about 1 min; it is possible that increasing the residence time would improve the dispersion.

Elongation at break for iPP/SiO_2 nanocomposites with untreated SiO_2 was about the same as that for neat iPP for all compositions (Fig. 5). In contrast, Rong et al.[35] found that as the amount of silica increased, elongation at break decreased. However, for the nanocomposites with surface-treated nanoparticles in the present study, a drastic decrease in elongation at break was observed. Thus, the tensile strength of the corresponding nanocomposite was low. The samples broke before stress hardening. Such a behavior is found only in reinforced plastics with sort glass fibers or after the addition of rigid inorganic large-sized particles.[41] So, apparently in our nanocomposites, the nanoparticles acted as rigid filler, reducing the ability of the polymer matrix for extension.

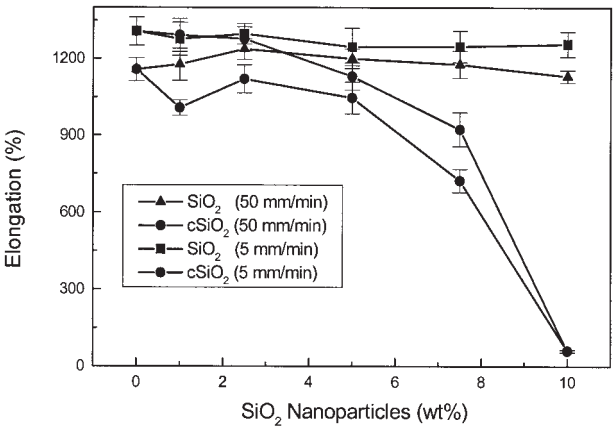

Figure 5 Elongation at break of iPP/SiO_2 nanocomposites at different crosshead speeds.

Estimation of interfacial adhesion

Among mechanical properties, tensile stress at the yield point of composites is of primary importance. It depends mainly on microstructure, including interfacial bonding as well as the form and size distribution of the filler, its spatial distribution in the matrix, the thickness of interface, and so forth. When there is poor bonding between matrix and filler, the applied load cannot be transferred to the filler, and thus the composite is brittle. For the iPP/SiO_2 nanocomposites of all compositions in the present study, the tensile strength at yield for those containing untreated silica was at the same levels as that of neat iPP, whereas for those containing surface-treated SiO_2, it was about 1–2 MPa higher. These higher values might be an indication of some adhesion of surface-treated SiO_2 with the polymer matrix. However, the picture was not the same when the values of tensile strength at break were compared because higher values were obtained for nanocomposites with untreated particles. For the interpretation of this last observation, perhaps other factors such as particle size and dispersion in the matrix also should be considered. For toughening of polymer/composites, it is believed that when tensile stress at break, σ_b, is lower than tensile strength at the yield point, σ_y, a brittle fracture occurs. When the opposite occurs, that is, when σ_b is higher than σ_y, then yielding will be the predominant deformation mechanism. The fracture in this case would be ductile. So, in the present study the nanocomposites prepared with untreated SiO_2 seemed to be ductile materials because tensile strength at break at all compositions was higher than tensile strength at the yield point. However, the nanocomposites containing surface-treated silica greater than 5 wt % became brittle material because tensile strength at break was lower that the corresponding tensile strength at the yield point.

Assuming poor adhesion between SiO_2 particles and iPP matrix for spherical particles such as the

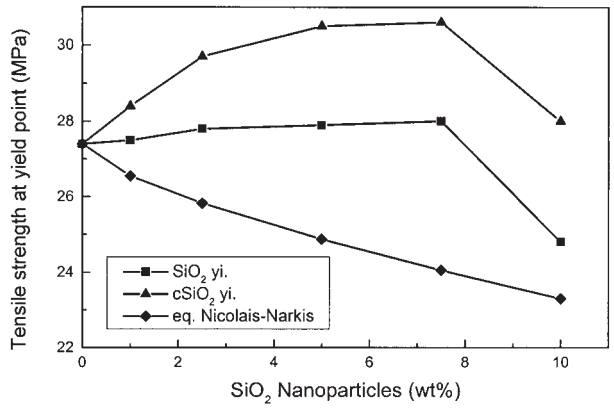

Figure 6 Comparison of calculated and experimental results of tensile strength at yield point.

nanosilica particles used in the present study, yield stress can predicted by the following equation proposed by Nicolais and Narkis[42]:

$$\sigma_{yc} = \sigma_{ym}(1 - 1.21\phi^{2/3}) \quad (1)$$

where σ_{yc} is the tensile stress at the yield point of the composite, σ_{ym} is the tensile stress at the yield point of the matrix, and ϕ is the volume fraction, which can be calculated using eq. (2)

$$\phi = \rho_m W_f/[(\rho_m - \rho_c)W_f + \rho_c] \quad (2)$$

where W_f is the weight fraction and ρ_m and ρ_c are the densities of the iPP (0.9 g/cm^3) and SiO_2 (2.2 g/cm^3) nanoparticles, respectively.

Figure 6 shows a comparison of the predicted values of yield stress according to the above equation with the values measured in the studied composites. The predicted values continuously decreased with an increasing amount of SiO_2. This usually was observed for composite materials, where adhesion between the different components was lacking. Furthermore, the experimental values in all compositions were higher than the theoretical values in both composites of untreated and treated particles. Even 10 wt % SiO_2, in which a slight drop also was observed in the experimental values, these values were still higher than the theoretical values. This might be an indication of some weak adhesion between iPP and SiO_2, which is more probable for dimethyldichlorosilane-treated nanoparticles. For untreated silica nanocomposites only weak van der Waals interactions can take place between SiO_2 and iPP, but these, according to Wu, are sufficiently strong to bear compatibility between the different materials, if an ordered crystalline interphase exists.[16,17] Finally, it seems that the Nicolais–Narkis equation may not be able to predict with accuracy variation in the yield stress of these nanocomposites, maybe because of the large specific area of the nanoparticles.

For when there is bonding between the matrix and the dispersed filler particles, Turcsányi et al.[43] introduced a new constant, B, to predict the extent of interfacial adhesion. Although this constant has no direct physical meaning, it obviously is connected with the interfacial properties of a particular system and also depends on the yield stress of the matrix. When B is greater than 3, interfacial bonding increases with increasing volume fraction. As can be seen in Figure 7, for iPP/untreated SiO_2 nanocomposites, the calculated values fit the experimental measurements well for $B = 9$, except for an SiO_2 content of 10 wt %. This means that despite the iPP being a hydrophobic polymer SiO_2 being a hydrophilic material because of its surface hydroxyl groups, a high degree of bonding should occur between them, as also was concluded by applying the Nicolais–Narkis equation. The value $B = 9$ in this case was even higher than that for similar iPP/SiO_2 composites ($B = 6$) with extremely small sizes (exact sizes not noted).[43] For surface-treated nanoparticles to better fit the experiment, even higher B values of 12 and 14 should be supposed, although even with $B = 12$ and $B = 14$, the fit was still not very satisfactory. For $B = 12$, as can be seen in Figure 7, for an SiO_2 content of up to 5 wt %, the experimental values were higher than the theoretical ones, whereas for 7.5 and 10 wt % silica, the trend was the opposite, with calculated values higher than measured values. For $B = 14$, a satisfactory prediction was found for up to 5 wt % SiO_2, whereas large deviations were observed for higher contents. However, a somewhat higher adhesion was found for surface-treated SiO_2 nanoparticles in the iPP matrix than for the untreated SiO_2. This equation also apparently provided better results than did that of Nicolais and Narkis:

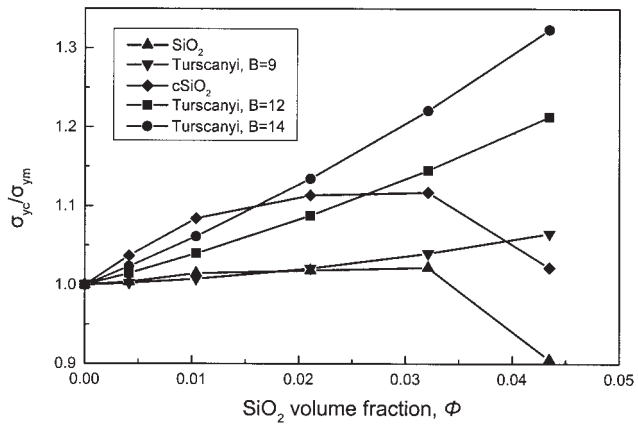

Figure 7 Relative yield stress of composites as a function of filler volume fraction compared with calculated values from eq. (3) with different constant values, B.

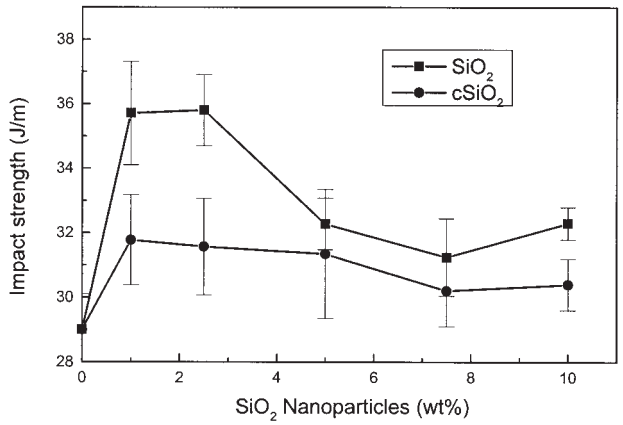

Figure 8 Impact strength of iPP and iPP/SiO_2 nanocomposites.

$$\sigma_{yc} = \frac{1 - \phi}{1 + 2.5\phi}\sigma_{ym} \exp(B\phi) \quad (3)$$

Impact strength and morphological characteristics

The effectiveness of nanoparticles to bear impact toughness has been widely investigated. It was found that the addition to iPP of small amounts of $CaCO_3$ nanoparticles (4.8 vol %) with an average particle size of 44 nm resulted in a significant increase, more than 500%, in notched fracture toughness.[32] In the iPP/SiO_2 nanocomposites of the present study, impact strength was found to be higher than of neat iPP (Fig. 8). Like the other mechanical properties already discussed, this depended, however, on both the kind and concentration of the silica nanoparticles used. Nanocomposites with untreated silica resulted in higher impact strength than did the use of those with treated SiO_2 at all compositions. Apparently the presence of large silica agglomerates reduced impact strength. However, in both types of silica nanocomposites, maximum impact strength was observed at concentrations of 1 and 2.5 wt %, concentrations at which the highest values of tensile strength also were detected. The impact strength of the nanocomposites increased about 20% for untreated SiO_2 and almost 10% for surface-treated SiO_2, compared with the iPP. Such observations of a particular weight fraction of filler for an optimum in mechanical performance also have been mentioned in other nanocomposite studies.[40,44,45] In all these studies, this optimization was a result of the effect of particle size rather than of particle dispersion.

From the SEM micrographs of the fractured specimen surfaces of the nanocomposites, a brittle surface, similar to that in neat iPP, was revealed (Fig. 9). Fibrils were not observed at any particle concentration. If fibrils had been observed, this would have been an indication of ductile behavior caused by the addition of SiO_2 nanoparticles. In the iPP/SiO_2 nanocomposites debonding cavities around the silica aggregates were observed, which were more profound at a concentration of 5 wt %. The formation of voids and the occurrence of particle debonding probably were the result of poor interfacial adhesion and the ductile behavior of the iPP matrix. It is well known from rubber toughening studies that when energy dissipation occurs in specimens, the morphological characteristics of the matrix are altered. Cavitation, inducing massive shear deformation, is the dominant mechanism in rubber toughening of thermoplastic polymers. Some authors claimed that this mechanism also controlled toughening in composites with inorganic fillers.[46,47] Chan et al.[32] found that the plastic massive deformation on the fracture surface of PP/$CaCO_3$ nanocomposites was accompanied by a large number of matrix voids. These clearly were caused by the addition of nanoparticles, and the matrix ligaments between the voids were stretched and deformed extensively. So cavitation-induced shear deformation is the most dominant mechanism for toughening in nanocomposites. However, for the nanocomposites in the present study, unless the increase in impact strength was small, there was no other indication of ductile behavior resulting from the addition of SiO_2.

From micrographs of Figure 9, it was concluded that there was a uniform dispersion of agglomerates in the matrix with high SiO_2 content. From a comparison of the micrographs of nanocomposites with 5, 7.5, and 10 wt % SiO_2 content to the corresponding ones for fracture after drawing, it was concluded that the agglomerates were reduced in size after the impact test. A

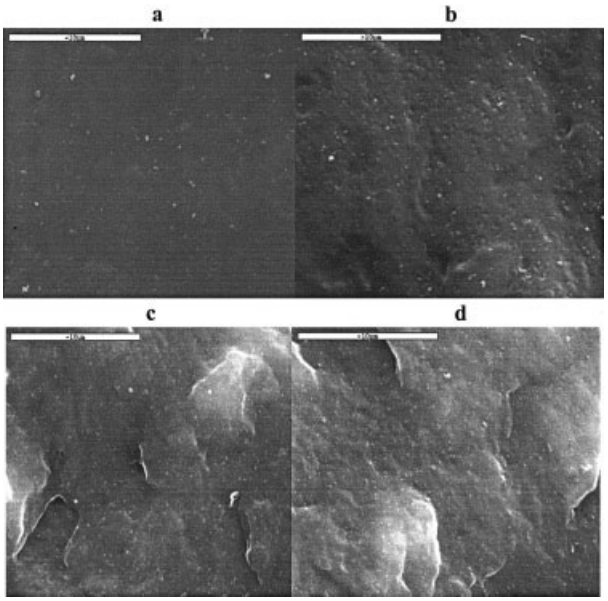

Figure 9 SEM micrographs of iPP/SiO_2 nanocomposites with different amounts of untreated SiO_2 derived from impact-fractured specimens: (a) 2.5 wt %, (b) 5 wt %, (c) 7.5 wt %, (d) 10 wt %.

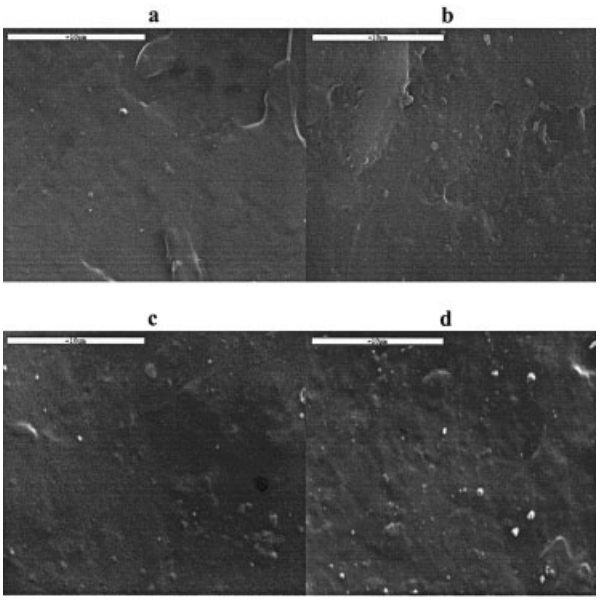

Figure 10 SEM micrographs of iPP/SiO_2 nanocomposites with treated SiO_2 derived from impact-fractured specimens: (a) 2.5 wt %, (b) 5 wt %, (c) 7.5 wt %, (d) 10 wt %.

probable explanation for this is that the agglomerates were broken down into smaller sizes as a result of energy absorption. Kim et al.[48] proposed such a mechanism comprising a multiple debonding process for silica aggregates in PE/SiO_2 composites. In this mechanism, stress concentration takes place in aggregates comprised of the soft particles during the deformation process. Because of the small interparticle distance, the shear flow process and fibrillation are activated inside the agglomerates, and the matrix between the aggregates deforms plastically, increasing toughness. If this were also true in iPP/SiO_2 nanocomposites, the specific samples (5, 7.5, and 10 wt %) should exhibit particularly high mechanical properties, higher than the impact strength of the nanocomposites with 1 or 2.5 wt %, but this was not the case. The same phenomenon was observed for samples with treated silica (Fig. 10). In the microphotographs of the treated nanocomposites, there were traces of aggregates much larger in size than there were in those of the untreated silica nanocomposites. This should have been associated with their lesser impact strength. However, in this case the aggregates were smaller than those on the surfaces of drawn specimens. Even with a 10 wt % content their size did not exceed 1 μm. To validate the applicability of Kim's theory, all samples were studied with TEM, with micrographs taken at higher magnification and the morphology as well as the agglomerations examined.

Figures 11 and 12 show the TEM images of iPP/SiO_2 nanocomposites containing different kinds and amounts of SiO_2. The brighter regions can be ascribed to the iPP matrix and the darker regions to the SiO_2 nanoparticles. It is obvious that nanoparticle dispersion in nanocomposites with lower SiO_2 content was more homogeneous than in nanocomposites with higher SiO_2 content. Nanoparticles that were mainly 10–12 nm in size aggregated to form clusters. However, these were not new entities, like the spheres observed in the SEM images, but remained individual, maintaining their original particle size. This shows

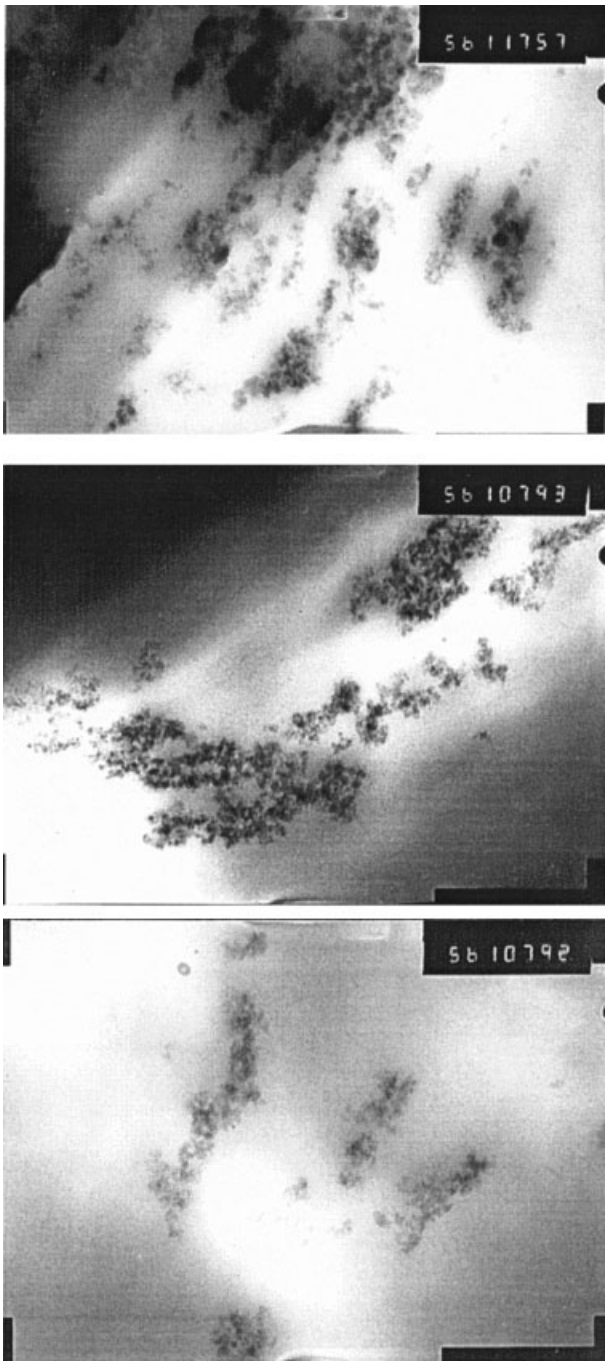

Figure 11 TEM micrographs of iPP/SiO_2 nanocomposites with different amounts of untreated SiO_2 derived from impact-fractured specimens containing different amounts of SiO_2: (a) 2.5 wt %, (b) 5 wt %, (c) 10 wt %.

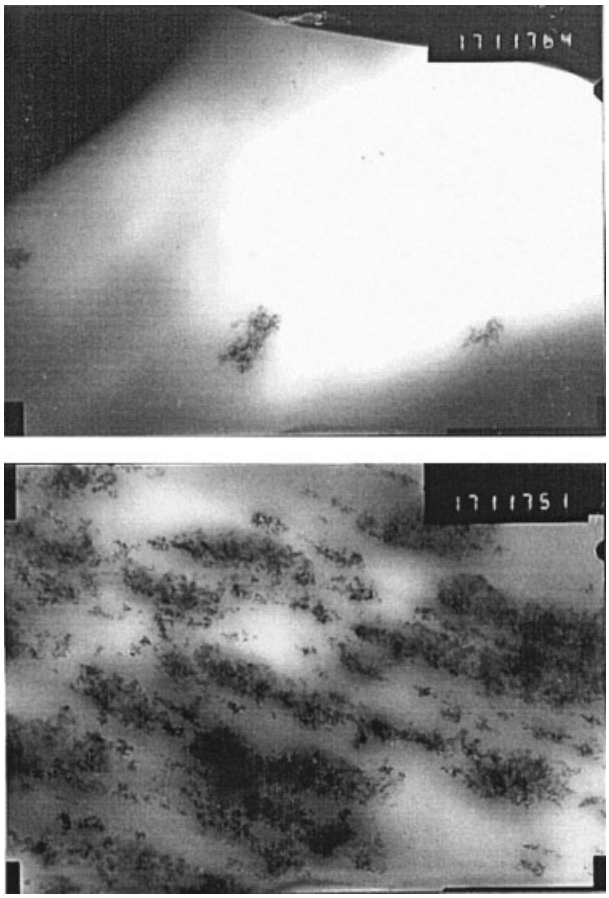

Figure 12 TEM micrographs of iPP/SiO_2 nanocomposites with treated SiO_2 derived from impact-fractured specimens containing different amounts of SiO_2: (a) 2.5 wt %, (b) 10 wt %).

that the initial aggregates were maintained almost unaltered during compounding via melt mixing. The shear forces developed in the extruder were not capable of splitting and uniformly propagating the nanoparticles into the polymer matrix. Also, the oblong form of the aggregates indicated that their orienting in the direction of polymer extrusion occurred. As can be seen in the TEM micrographs, nanocomposites with smaller amounts of nanosilica particles were finely dispersed on a nanometer-size scale. However, even in this case, some aggregates, more than 100 nm in size, were formed. As the amount of nanosilica increased in the iPP matrix, these aggregates predominated, forming clusters, whereas dispersion of single nanoparticles failed. An examination of the inside of the agglomerates showed no fibrillation in any sample, unlike what Kim et al. proposed.[48] Finally, it was also verified by TEM that the treated SiO_2 nanoparticles created larger agglomerates (Fig. 12) than did the untreated ones.

Interparticle distance

According to Wu, the critical interparticle distance is a material property of the matrix, and consequently, toughening can be achieved if this criterion is satisfied, by the addition of either elastomers or hard inorganic fillers.[16] However, the results obtained after the addition of elastomers and inorganic fillers into the same polymer matrix. For example, in polyoxymethylene (POM) toughening with an elastomer, it was found that interparticle distance was about 0.2 μm,[22] which is very close to the distance (0.18 μm) reported for the same polymer in another case.[21] Furthermore, when ternary composites containing different amounts and particle sizes of $CaCO_3$ as inorganic filler were prepared, critical ligament thickness increased to 0.56 μm. Thus, it seems that perhaps critical ligament thickness is not a material parameter or better internal property, as most researchers claimed. Reports concerning the applicability of the critical interparticle distance criterion for toughening, specifically in nanocomposites, are very limited. Thus, in this work an effort was made to explore the applicability of this criterion in such a case.

For the calculation of the critical interparticle distance (ID), eq. (4), proposed by Wu,

$$\mathrm{ID} = d[(\pi/6\phi)^{1/3} - 1] \tag{4}$$

was used, and the resulting values of ID versus impact strength are presented in Figure 13. Using the particle diameter (d = 12 nm), the value corresponding to the point where a sharp increase in impact strength appeared was found to be less than 20 nm. This distance is close to the sum of diameters of two particles. Wu[16,17] claimed that when there is a sufficient interpenetration of the plastic zones formed around the particles, propagation of the microcrackings in the matrix does not occur but instead drastically inhibited. This may result in a substantial increase in impact strength. But, in fact, morphological examination of nanocomposites with SEM and TEM, showed that only a limited number of the original particles still

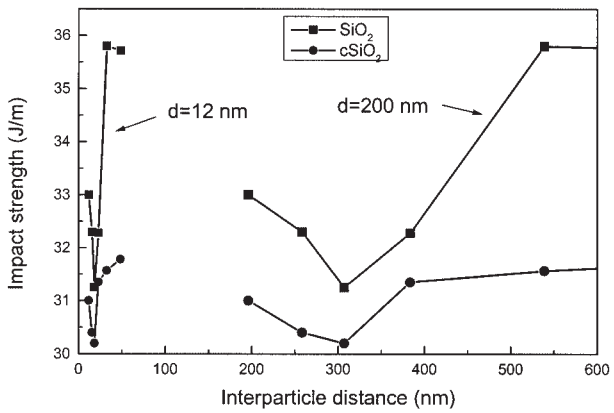

Figure 13 Impact strength versus interparticle distance of iPP/SiO_2 nanocomposites.

TABLE I
Variation of Thermal Properties and Degree of Crystallinity of iPP/SiO_2 Nanocomposites

	Untreated silica					Surface-treated silica				
SiO_2 (wt %)	T_m (°C)	T_c (°C)	ΔH_c (J/g)	ΔH_m (J/g)	X_c (%)	T_m (°C)	T_c (°C)	ΔH_c (J/g)	ΔH_m (J/g)	X_c (%)
0	162.1	111.4	90.0	91.1	62.8	162.1	111.4	90.0	91.1	62.8
1	161.7	111.7	89.9	90.9	62.7	162.0	111.6	90.9	91.3	62.9
2.5	160.0	111.9	90.0	90.2	62.2	160.6	112.6	88.0	88.8	61.2
5	160.2	112.5	93.6	94.0	64.8	161.0	113.1	92.0	93.0	64.1
7.5	161.0	114.4	97.0	98.8	68.1	161.5	112.9	96.1	97.5	67.2
10	161.0	114.0	97.8	100.8	69.5	161.3	113.7	97.1	98.4	67.9

existed, and agglomerates were mostly observed. Thus, the original particle diameter should not be used. Because the average aggregate size ranged between 150 and 250 nm, a diameter of about $d = 200$ nm probably should be accepted. As shown in Figure 13, assuming $d = 200$ nm, for both nanocomposite types (with treated or untreated silica), the abrupt increase in impact strength corresponded to an interparticle distance of about 300 nm. Thus, there is in agreement with Wang et al., as they reported that for iPP, ID should be below 420 nm.[20] Of course, there are still some open issues. The average aggregate diameter depends on aggregate concentration and particle treatment. For treated particles, it could be supposed that there would be an even larger diameter, resulting in larger interparticle distance. Furthermore, though such a value was in agreement with SEM observations, with nanocomposites with a silica content greater than 5 wt %, no increase in impact strength was observed, in contrast to what was anticipated. In contrast, the calculated critical interparticle distance was 200 or 100 nm lower than the observed particle distance for nanocomposites with 1 and 2.5 wt %, respectively, for which higher impact strength was found. For precise estimations of critical interparticle distance in nanocomposites, nanoparticles should have a definite size as a result of good dispersion in the matrix and the absence of aggregates.

Thermal properties

Because the addition of the nanoparticles was not expected to affect the molecular weight or to cause any chain branching in iPP, which might influence the crystalline phase of iPP in the nanocomposites, only the nucleating activity of the nanoparticles was to be considered.[49] A careful study of the melting peaks in the DSC traces of the nanocomposites recorded after the same thermal treatment led to the conclusion that the peak temperatures were reduced by about 1°C–2°C compared with that for the neat iPP. It should be noted that the lowest value was for nanocomposites containing 2.5 wt % SiO_2 in both treated and untreated nanoparticles. The point is, with this SiO_2 content, greater increases in tensile strength at break and in impact strength were observed. Thus, for this concentration, the supposition was that interactions between the polymer matrix and the nanoparticles occurred to a greater extent. The melting point of polymer crystals is a function of lamellar thickness and the degree of perfection. Consequently, this reduction of T_m should be associated with reduced crystal size and/or crystal defects, which are both results of increased crystallization rates from the nucleating activity of the nanoparticles.

As can be seen in Table I, the crystallinity of the samples obtained after cooling at 20°C/min was constant for nanoparticles with a silica content of up to 2.5 wt %. For higher silica content, crystallinity increased up to 10%, whereas the melting temperatures decreased about 1°C–2°C, independent of the concentration of nanoparticles. The enhanced effect of SiO_2 on crystallization rates also can be seen from the crystallization temperature—increasing the silica amount moved the values close to the melting point. This means that PP crystallization became faster. A comparison of samples containing treated and untreated particles showed that the increase was less in treated nanoparticles. An analogous behavior was recently reported for HDPE/$CaCO_3$ composites, in which the calcium carbonate particles influenced nucleation of polyethylene crystallites by increasing the crystallization temperature.[24] The influence depended on surface treatment and particle size. In all cases a substantial increase in the degree of crystallinity of up to 8% was observed by increasing the $CaCO_3$ content and especially by reducing the particle size (in other words, by increasing the specific area). However, in all composites the melting point shifted to lower temperatures, demonstrating that the lamellae thickness was lower than in neat HDPE. However, some studies reported opposite findings, for example, with iPP/silver nanocomposites.[33]

Figure 14 shows the melting peaks of the nanocomposites. There were differences in the shape of the peaks between the nanocomposites and the pure iPP.

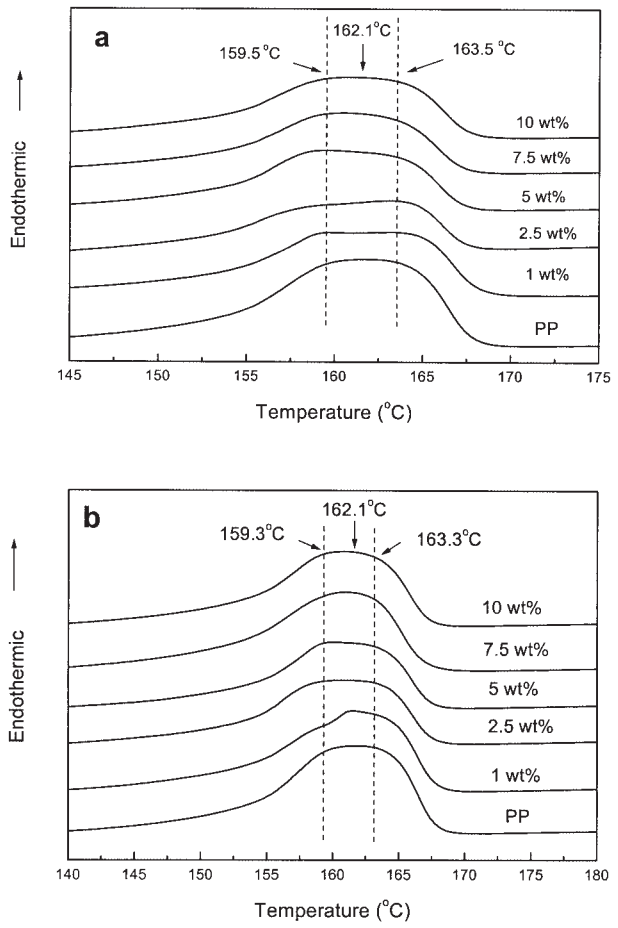

Figure 14 Melting peaks of iPP and its nanocomposites: (a) untreated SiO_2, (b) surface-treated SiO_2.

For the nanocomposites the melting peaks were rather complex and probably were the sum of the overlapping of two peaks. In other words, in the nanocomposites the melting of different or broader crystal distributions is observed. Differences in general may have been a result of crystal form, size, or perfection. It is known that isotactic polypropylene can crystallize in three forms: the monoclynic α-form, the hexagonal β-form, and the triclinic γ-form.[50] In normal processing conditions, the α phase is the principal constituent, which may be accompanied by a relatively small amount of the β phase. However, the formation of the β phase can be promoted in iPP by adding various inorganic particles such as calcium carbonate or wollastonite, which can act as nucleators.[51,52] So according to this, because SiO_2 nanoparticles act as nucleating agents for iPP,[49] the formation of a β-polymorph in our nanocomposites could have taken place. It should be noted here that these polymorphs had different effects on the mechanical properties of PP, and for this reason it is very important to identify if they were present in our prepared iPP nanocomposites. Under tensile loading, α-spherulites exhibit brittle behavior, whereas the β phase deforms plastically up to high deformations.[53] These different iPP modifications were easily detected from differential scanning calorimetry (DSC). Schneider et al. observed two peaks, one at about 162°C–165°C, which was attributed to the α-polymorph of iPP, and a second peak at 151°C–54°C, which was interpreted as the melting of the β-polymorph.[54] However, in our nanocomposites the two peaks observed were close to each other, at temperatures higher than 158°C. In that case the peak of the low melting temperature should be associated with the less stable $\alpha 1$ phase of iPP, which after recrystallization transforms into the more stable phase, $\alpha 2$.[55]

CONCLUSIONS

iPP/SiO_2 nanocomposites with untreated and surface-treated silica nanoparticles were prepared by melt compounding using a corotating screw extruder designed especially for iPP composite preparation. SiO_2 contents of 1, 2.5, 5, 7.5, and 10 wt % were used. All nanocomposites were transparent as pure iPP, indicating fine dispersion of the silica nanoparticles into iPP matrix and the retention of their nanosizes. However, scanning and transmission electron microcopy indicated that silica nanoparticles were dispersed not as individual particles but more or less as agglomerates. The extent of the agglomeration depended on the amount of SiO_2 as well as on its hydrophobic or hydrophilic character.

After morphological examination of the surface of the fracture in the nanocomposite specimens caused by drawing or impact, the relationship between the characteristics and the mechanical properties of the structure gained was more obvious. These property enhancements were controlled mainly by the extension of SiO_2 agglomeration. Using the equation of Turcsányi et al.,[43] it was found that interfacial adhesion to the iPP matrix was higher with surface-treated silica.[43] However, the mechanical properties of these nanocomposites were lower than the corresponding ones of the nanocomposites containing untreated silica. However, in both case it appears that the mixing time during extrusion was not sufficient to achieve a fine dispersion of the SiO_2 nanoparticles into the iPP matrix.

Thermal analysis of the nanocomposites revealed that SiO_2 is an effective nucleating agent. PP crystallinity increased by increasing the filler content.

References

1. Nothon, R. N. Adv Polym Sci 1999, 139, 67.
2. Nezbedova, E.; Ponesicky, J.; Sova, M. Acta Polymerica 1990, 41, 36.
3. Mitsuishi, K. Ang Makrom Chem 1997, 248, 73.

4. Osman, M. A.; Atallah. A.; Suter, U. W. Polymer 2004, 45, 1177.
5. Mitsuishi, K.; Kodama, S.; Kawasaki, H. Polym Eng Sci 1985, 25, 1069.
6. Mareri, P.; Bastide, S.; Binda, N.; Crespy, A. Compos Sci Technol 1998, 58, 747.
7. Svehlova, V.; Poloucek, E. Angew Makromol Chem 1987, 153, 728.
8. Tabtiang, A.; Venales, R. Eur Polym J 2000, 36, 137.
9. Argon, A. S.; Cohen, R. E. Polymer 2003, 44, 6013.
10. Wilbrink, M. W. L.; Argon, A. S.; Cohen, R. E.; Weinberg, M. Polymer 2001, 42, 10155.
11. Pukanszky, B. In Polypropylene: Structure, Blends and Composites; Vol. 3, Composites; Karger-Kocsis, J., Eds., Chapman & Hall: London, 1995.
12. Wang, Y.; Lu, J.; Wang, G. J Appl Polym Sci 1997, 64, 1275.
13. Fu, Q.; Wang, G.; Shen, J. J Appl Polym Sci 1993, 49, 673.
14. Nezbedova, E.; Ponesicky, J.; Sova, M. Acta Polymerica 1990, 41, 36.
15. Dompas, D.; Groeninckx, G. Polymer 1994, 35, 4743.
16. Wu, S. Polymer 1985, 26, 1855.
17. Wu, S. J Appl Polym Sci 1988, 35, 549.
18. Bartczak, Z.; Argon, A. S.; Cohen, R. E.; Weinberg, M. Polymer 1999, 40, 2331.
19. Wu, X.; Zhu, X.; Qi, Z. in 8th International Conference on Deformation, Yield and Fracture of Polymers. London: Plastics and Rubber Institute, 1991.
20. Wang, Y.; Fu, Q.; Li, Q.; Zhang, G.; Shen, K.; Wang, Y. Z. J Polym Sci, Part B: Polym Phys 2002, 40, 2086.
21. Kanai, K.; Sullivan, V.; Auerbach, A. J Appl Polym Sci 1994, 53, 527.
22. Gao, X.; Qu, C.; Zhang, Q.; Peng, Y.; Fu, Q. Macromol Mater Eng 2004, 289, 41.
23. Loyens, W.; Groeninckx, G. Polymer 2003, 44, 123.
24. Bartczak, Z.; Argon, A. S.; Cohen, R. E.; Weinberg, M. Polymer 1999, 40, 2347.
25. Bartczak, Z.; Argon, A. S.; Cohen, R. E.; Kowalewski, T. Polymer 1999, 40, 2367.
26. García-López, D.; Picazo, O.; Merino, J. C.; Pastor, J. M. Eur Polym J 2003, 39, 945.
27. Hasegawa, N.; Okamoto, H.; Kato, M.; Usuki, A. J Appl Polym Sci 2000, 78, 1918.
28. Tang, Y.; Hu, Y.; Song, L.; Zong, R.; Gui, Z.; Chen, Z.; Fan, W. Polym Degrad Stab 2003, 82, 127.
29. Xu, W.; Liang, G.; Zhai, H.; Tang, S.; Hang, G.; Pan, W.P. Eur Polym J 2003, 39, 1467.
30. Saujanya, C.; Radhakrishnan, S. Polymer 2001, 42, 6723.
31. Wu, C. L.; Zhang, M. Q.; Rong, M. Z.; Friedrich, K. Comp Sci Technol 2002, 62, 1327.
32. Chan, C. M.; Wu, J.; Li, J. X.; Cheung, Y. K. Polymer 2002, 43, 2981.
33. Yeo, S. Y.; Jeong, S. H. Polym Int 2003, 52, 1053.
34. Lehmann, B.; Friedrich, K.; Wu, CL.; Zhang, M. Q.;, Rong, M. Z. J Mater Sci Lett 2003, 22, 1027.
35. Rong, M. Z.; Zhang, M. Q.; Zheng, Y. X.; Zeng, H. M.; Walter, R.; Friedrich, K. Polymer 2001, 42, 167.
36. Rong, M. Z.; Zhang, M. Q.; Pan, S. L.; Lehmann, B.; Friedrich, K. Polym Int 2004, 53, 176.
37. Ikeda, Y., Kohjiya, S. Polymer 1997, 38, 4417.
38. Canevaro, S.; Candia, F. J Appl Polym Sci 1995, 57, 533.
39. Yanh, F.; Ou, Y.; Yu, Z. J Appl Polym Sci 1998, 69, 355.
40. Ash, B. J.; Siegel, R. W.; Schadler, L. S. Macromolecules 2004, 37, 1358.
41. Bikiaris, D.; Matzinos, P.; Flaris, V.; Larena, A.; Panayiotou, C. J Appl Polym Sci 2001, 81, 701.
42. Nicolais, L.; Narkis, M. Polym Eng Sci 1971, 11, 194.
43. Turcsányi, B.; Pukánszky, B.; Tüdõs, F. J Mater Sci Lett 1988, 7, 160.
44. Qu, Y.; Yang, F.; Yu, Z. J Polym Sci, Part B: Polym Phys 1998, 36, 789.
45. Zhang, J.; Wang, X.; Lu, L.; Li, D.; Yang, X. J Appl Polym Sci 2003, 87, 381.
46. Pearson, R. A.; Yee, A. F. J Mater Sci 1989, 24, 2571.
47. Parker, D. S.; Sue, H. J.; Huang, J.; Yee, A. F. Polymer 1990, 31, 2267.
48. Kim, G. M.; Michler, G. H. Polymer 1998, 39, 5699.
49. Papageorgiou, G. Z.; Achilias, D. S.; Bikiaris, D. N.; Karayannidis, G. P. Thermochimica Acta, in press.
50. Verga, J. J Mater Sci 1992, 27, 2557.
51. Liu, J.; Wie, X.; Guo, Q. J Appl Polym Sci 1990, 41, 2829.
52. McGenity, P. M.; Hooper, J. J.; Paynter, C. D.; Riley, A. M.; Nutbeem, C.; Elton, N. J.; Adams, J. M. Polymer 1992, 33, 5215.
53. Aboulfaraj, M.; G'Sell, C.; Ulrich, B.; Dahoun, A. Polymer 1995, 36, 731.
54. Schneider, K.; Zafeiropoulos, N. E.; Häubler, L.; Stamm, M. Macrom Rapid Commun 2004, 25, 355.
55. Boudenne, A.; Ibos, L.; Fois, M.; Gehin, E.; Majeste, J. C. J Polym Sci, Part B: Polym Phys 2004, 42, 722.